Te—Te Bonding in Copper Tellurides

Seeyearl Seong,[1] Thomas A. Albright,*[,1] Xiang Zhang,[2] and Mercouri Kanatzidis*[,2]

Contribution from the Department of Chemistry and Texas Center for Superconductivity at the University of Houston, University of Houston, Houston, Texas 77204-5641, and Department of Chemistry, Michigan State University, East Lansing, Michigan 48824

Received March 18, 1994®

Abstract: Tight binding calculations at the extended Hückel level have been used to study the bonding in NaCuTe, $K_2Cu_5Te_5$, and CuTe. NaCuTe is predicted to be a semiconductor with the lowest band gap at Γ. The highest filled orbitals are tellurium centered, and the lowest unoccupied orbitals are derived from Cu s. $K_2Cu_5Te_5$ is metallic; the holes at the Fermi level are Te p_y based (parallel to the *a* direction) and are delocalized equally over the three different Te sites. The reduction of $K_2Cu_5Te_5$ by one electron is not expected to yield a semiconductor; a structural distortion is anticipated which will break Te—Te bonds. CuTe is predicted to be also metallic at the experimentally established geometry. An alternative structure where Te—Te bond pairing occurs has been optimized and found to be at a slightly lower energy than the experimental one. This pairing is predicted to open a band gap. However, experiment shows no evidence for a metal insulator transition down to 5 K. The reasons for why the extended Hückel method fails to correctly order these two structures in terms of energy are probed.

Indications of the existence of CuTe were found as early as 1908 by Pushkin,[3] who studied the Cu—Te system by potentiometric methods. This was confirmed by Anderco and Schuber,[4,5] and the structure was refined by Baranova and Pinsker.[6] This compound is also known as the mineral vulcanite. The binary transition metal monochalcogenides, especially the sulfides and selenides, have received considerable attention because of their interesting electrical and magnetic properties;[7-9] however, not much is known about CuTe itself. The existence of stoichiometric CuTe is, in fact, quite rare in the Cu—Te system.[10] Differential thermal analysis and X-ray diffraction revealed[11] that CuTe disproportionates at 340 °C into $Cu_{3-x}Te_2$ and a telluride-rich melt. Many other techniques have been used to study the properties of the nonstoichiometric Cu—Te system.[12]

Our interest in CuTe was sparked by its relationship to NaCuTe[13] and a new ternary CuTe phase, $K_2Cu_5Te_5$, which has been reported in a preliminary communication.[14] In each of these three compounds the copper atoms are centered on tetrahedral sites and the tellurium atoms are coordinated in a square pyramidal fashion to four copper atoms. In NaCuTe the formal oxidation states are Cu(+1) and Te(-2), and therefore, it is not surprising that this compound is a semiconductor. The other two compounds are electron deficient. For metal tellurides it has been recognized in a variety of contexts[15-18] that often the electron deficiency resides primarily on the tellurium atoms rather than on the metal. This electron deficiency can be totally, or partially, relieved by the formation of Te—Te bonds. Thus, for $K_2Cu_5Te_5$ one Te—Te bond is formed, and a more descriptive formula for this material is $K_2Cu_5(Te_2)Te_3$.[14] This leaves one hole per formula unit. The basic structure[6] of CuTe is close to that of NaCuTe except that there is a lattice compression along [100] leading to the formation of straight, parallel Te chains with Te—Te distances in the *a* direction of 3.15 Å, while those in the *b* direction are 4.09 Å. $CuAgTe_2$ has been reported[19] to be isostructural to CuTe; however, we are not aware of any other isoelectronic metal chalcogenides which possess this structural type. The questions that we will address in this work can be summarized as follows: (1) Where does the remaining hole localize (or delocalize) in $K_2Cu_5Te_5$? (2) Is it possible to add or remove an electron from $K_2Cu_5Te_5$, yielding $K_3Cu_5Te_5$ or KCu_5Te_5, respectively, and would this lead to a band gap? (3) Is CuTe a metal or a semiconductor; does the compression of CuTe along the *a* axis create a band gap? (4) Is there an alternative structural distortion in CuTe which will pair tellurium atoms? To examine these issues, we have employed tight binding calculations with an extended Hückel Hamiltonian.[20] Computational details are given in the Appendix.

• Abstract published in *Advance ACS Abstracts*, July 1, 1994.

(1) University of Houston.

(2) Michigan State University.

(3) Pushkin, N. *Z. Anorg. Allg. Chem.* **1908**, *56*, 1.

(4) Anderko, K.; Schubert, K. *Z. Metallkd.* **1954**, *45*, 371.

(5) Schubert, K.; Anderko, K.; Kluge, M.; Buskow, H.; Dorre, E.; Essl, P. *Naturwissenschaften* **1953**, *40*, 269.

(6) (a) Baranova, R. V.; Pinsker, Z. G. *Zh. Strukt. Khim.* **1970**, *11*, 690. (b) Baranova, R. V.; Pinsker, Z. G. *Kristallografiya* **1973**, *18*, 1169.

(7) (a) Hulliger, F. In *Structural Chemistry of Layered-Type Phases*; Levy, F., Ed.; D. Reidel: Dordrecht, 1976; Vol. 5. (b) Baranova, R. V.; Pinsker, Z. G. *Sov. Phys.-Crystallogr.* **1964**, *9*, 83. (c) De Medicis, R. *C. R. Seances Acad. Sci.* **1971**, *272D*, 513. (d) Arunsingh, O. N. S.; Dayal, B. *Acta Crystallogr.* **1972**, *B28*, 635. (e) Bertaut, E. F.; Burlet, P.; Chappert, J. *Solid State Commun.* **1965**, *3*, 335. (f) Takeno, S.; Zoka, H.; Niihara, T. *Am. Mineral* **1970**, *55*, 1639. (g) Hulliger, F. *Struct. Bonding* **1968**, *4*, 83. (h) Kjekshus, A. *Acta Chem. Scand.* **1973**, *27*, 1452. (h) Dvoryankina, G. G.; Pinsker, Z. G. *Sov. Phys.-Crystallogr.* **1963**, *8*, 448.

(8) (a) Bither, T. A.; Bouchard, R. J.; Cloud, W. J.; Donohue, P. C.; Siemons, W. J. *Inorg. Chem.* **1968**, *7*, 2208. (b) Abdullaev, G. B.; Aliyarova, Z. A.; Asadov, C. A. *Phys. Status Solidius* **1967**, *21*, 461.

(9) (a) Agarwal, B. K.; Verma, L. P. *J. Phys. C: Solid State Phys.* **1968**, *1*, 1658. (b) Bhide, V. G.; Bahl, M. K. *J. Chem. Phys.* **1970**, *52*, 4093; *J. Phys. Chem. Solids* **1971**, *32*, 1001. (c) Goodenough, J. B. *Bull. Soc. Chim. Fr.* **1965**, 1200.

(10) (a) Baranova, R. V.; Efremov, E. N. *Izv. Akad. Nauk SSSR, Neorg. Mater.* **1974**, *12*, 23. (b) Blacknik, R.; Lasocka, M.; Walbrecht, U. *J. Solid State Chem.* **1983**, *48*, 431.

(11) Stevel, A. L. N.; Wiegers, G. A. *Recl. Trav. Chim. Pays-Bas* **1971**, *90*, 352.

(12) (a) Prikhod'ko, E. V.; Sidorenko, K. Yu.; Kol'tsov, V. B. *Russ. J. Phys. Chem.* **1988**, *62*, 34. (b) Bahl, M. K. *J. Phys. C* **1978**, *8*, 4107. (c) Enderby, J. E.; Barnes, A. C. *Z. Phys. Chem.* **1988**, *156*, S. 529. (d) Burkhanov, A. S.; Saleeva, N. M. *Zh. Fiz. Khim.* **1975**, *49*, 1658. Makarov, G. V.; Batrakov, V. V. *Zh. Fiz. Khim.* **1990**, *64*, 2191. (e) Hanus, F.; Wautlet, M. *J. Appl. Phys.* **1990**, *68*, 3307.

(13) Sabelsberg, G.; Schafer, H. *Z. Naturforsch.* **1978**, *33B*, 370.

(14) Park, Y.; DeGroot, D. C.; Schindler, J.; Kannewurf, C. R.; Kanatzidis, M. G. *Angew. Chem., Int. Ed. Engl.* **1991**, *30*, 1325.

(15) (a) Canadell, E.; Jobic, S.; Brec, R.; Rouxel, J. *J. Solid State Chem.* **1992**, *98*, 59. (b) Canadell, E.; Whangbo, M.-H. *Inorg. Chem.* **1990**, *29*, 1398. (c) Jobic, S.; Deniard, P.; Brec, R.; Rouxel, J.; Jouanneaux, A.; Fitch, A. N. *Z. Anorg. Allg. Chem.* **1991**, *598/599*, 199. (d) Jobic, S.; Brec, R.; Rouxel, J. *J. Solid State Chem.* **1992**, *96*, 169. (e) Lee, S.; Hoistad, L. M.; Kampf, J. *New J. Chem.* **1992**, *16*, 657. (f) Mar, A.; Jobic, S.; Ibers, J. A. *J. Am. Chem. Soc.* **1992**, *114*, 8963. (g) Whangbo, M.-H.; Canadell, E. *Ibid* **1992**, *114*, 9587. (h) Ansari, M. A.; Bollinger, J. C.; Ibers, J. A. *Ibid.* **1993**, *115*, 3838.

(16) (a) Canadell, E.; Mathey, Y.; Whangbo, M. H. *J. Am. Chem. Soc.* **1988**, *110*, 104. (b) Jobic, S.; Brec, R.; Rouxel, J. *J. Solid State Chem.* **1992**, *98*, 59.

(17) Gressier, P.; Whangbo, M. H. *Inorg. Chem.* **1984**, *23*, 1228. Canadell, E.; Monconduit, L.; Evain, M.; Brec, R.; Rouxel, J.; Whangbo, M.-H. *Ibid.* **1993**, *32*, 10.

(18) Mitchell, J. F.; Burdett, J. K.; Keane, P. M.; Ibers, J. A.; Degroot, D. C.; Hogan, J. P.; Schindler, J. L.; Kannewurt, C. R. *J. Solid State Chem.* **1992**, *99*, 103.

(19) Avilov, A. S.; Baranova, R. V. *Sov. Phys.-Crystallogr.* **1972**, *17*, 180.

0002-7863/94/1516-7287$04.50/0

Chart 1

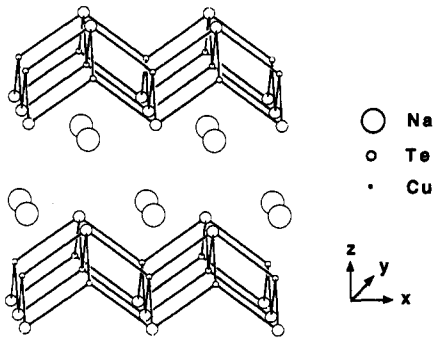

Chart 2

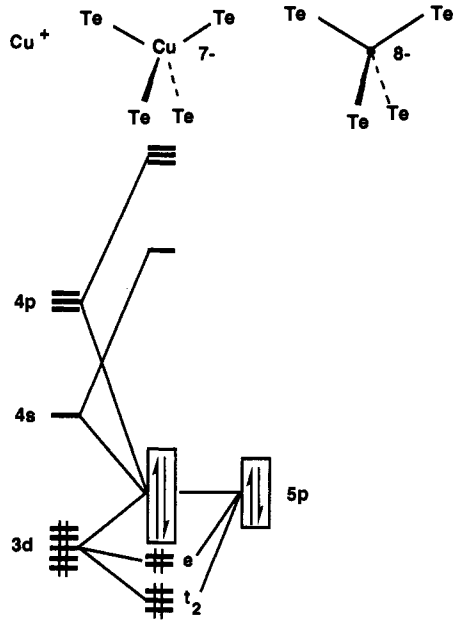

NaCuTe

NaCuTe is tetragonal with $P4/nmm$ symmetry.[13] The basic structure is illustrated in Chart 1. The CuTe layers are formed by edge-sharing $[Cu_2Te_2]$ unit cells to form the well-known anti-PbO type of structure. The local coordination geometry around copper is very close to tetrahedral, with Te—Cu—Te bond angles of 108.2° and Cu—Te bond lengths of 2.70 Å. The $CuTe_4$ tetrahedron propagates a two-dimensional layer by sharing four of its edges. Notice that there is a double layer of sodium cations between the CuTe layer; certainly, there is no significant interlayer interaction between the CuTe layers. Likewise, the Cu—Cu and Te—Te distances of 2.70 and 4.38 Å, respectively, preclude any interaction between these atoms within the CuTe layer.

As implied by the discussion concerning electron deficiency in the introduction, the tellurium p atomic orbitals are expected to lie slightly higher in energy than the copper d orbitals. Thus, the idealized interaction diagram given in Chart 2 can be constructed from the perspective of a single tetrahedron. The natural tetrahedral d orbital splitting pattern is reversed. The t_2 set at the metal is Cu—Te σ bonding and therefore stabilized more than the e set, which is Cu—Te π bonding. The tellurium 5p atomic orbitals are represented in Chart 2 by a block. They are antibonding with respect to copper 3d, but also significant amounts of copper 4s and 4p mix into these orbitals in a bonding fashion. Finally, the copper 4s and 4p orbitals are destabilized by the tellurium 5p set. These patterns are confirmed in the DOS (density of states) plots presented in Figure 1 for a $CuTe^-$ layer.

(20) (a) Hoffmann, R. *J. Chem. Phys.* **1963**, *39*, 1397. (b) Hoffmann, R.; Lipscomb, W. N. *Ibid.* **1962**, *36*, 2197. (c) Whangbo, M.-H.; Hoffmann, R.; Woodward, R. B. *Proc. R. Soc. London, Ser. A* **1979**, *366*, 23.

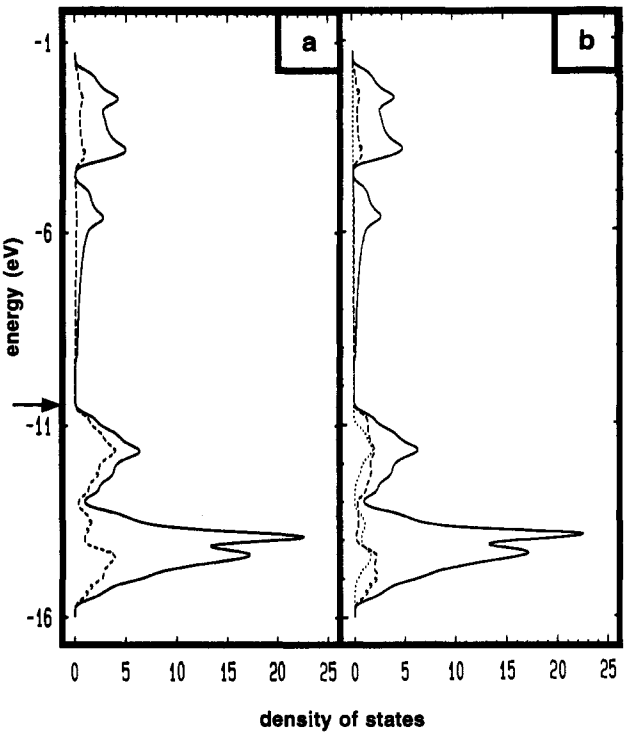

Figure 1. (a) total density of states (DOS) for a $CuTe^-$ layer. The dashed line indicates the projection of the tellurium orbitals. The arrow indicates the position of the highest filled orbitals. (b) Projection of the Te p_x and p_y (dashed line) and Te p_z (dotted line) orbitals.

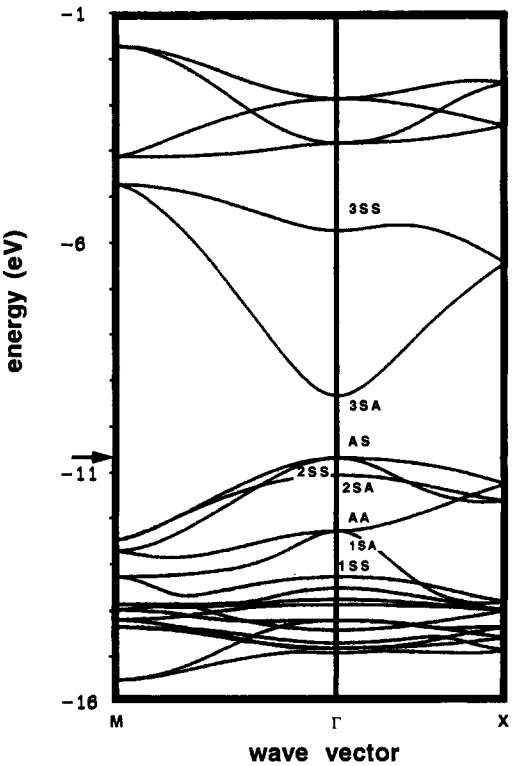

Figure 2. Band structure of a $CuTe^-$ layer. The arrow indicates the top of the highest filled band.

The sodium cations will interact in an electrostatic fashion and thus have been neglected in the computation. We should note that precisely the same DOS plot results when a full three-dimensional calculation was carried out, confirming the expectation that there is insignificant band dispersion between the layers. The full DOS curve in Figure 1a is given by the solid line. The dashed line indicates the projection of tellurium orbitals. The rather broad peak centered at −11.8 eV is primarily tellurium p

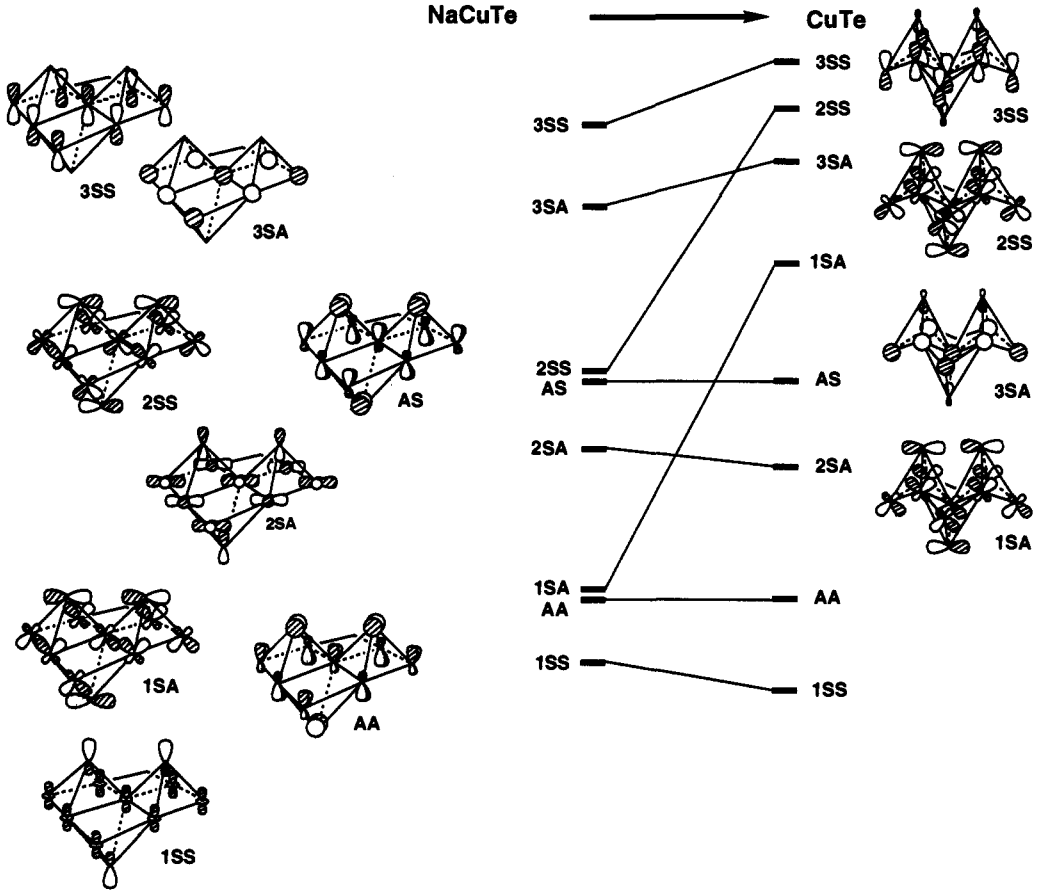

Figure 3. Orbital calculation diagram for going from the NaCuTe (left) to CuTe (right) type of structure. The form of the crystal orbitals is shown at the Γ point.

in character. The two large peaks at −14.0 and −14.5 eV are predominately copper d based orbitals. There is considerable tellurium character in the latter identifying it as the t_2 set, and consequently the peak at −14.0 eV is largely constructed from the e set for the tetrahedral splitting pattern presented in Chart 2. The tellurium p region is decomposed further in Figure 1b, where the Te p_x and p_y projections to the DOS are indicated by a dashed line and the Te p_z projection by a dotted line. The coordinate system used here is indicated in Chart 1. Notice that the dispersion associated with Te p_z is considerably smaller around −11.8 eV than that for Te p_x and p_y. The arrow on the left side of Figure 1a shows the position of the highest filled orbitals. The peak at −5.6 eV with a long tail toward lower energies is largely Cu s in character. We compute a band gap of 1.10 eV.

For comparison purposes in the next section, let us investigate in more detail the band structure of the $CuTe^-$ layer. The result of a two-dimensional calculation is given in Figure 2. There are two formula units per unit cell, and therefore, the 10 bands at lowest energy are associated with the Cu d block (at even lower energy and not shown in this figure are the two Te 5s bands). The six Te-based bands are labeled as being S or A (symmetric or antisymmetric, respectively) with respect to two symmetry elements that are present at the Γ point: the *xz* (*ab*) mirror plane and the glide plane lying along the *xy* direction(⟨110⟩), respectively. The construction of these crystal orbitals is explicitly drawn on the left side of Figure 3 at the Γ point. For visual simplicity the hybridization brought by Cu s and p has not been included in the drawings for 1SS and 2SA. The six Te p bands fall neatly into two groups at Γ. The 1SS crystal orbital is largely Cu—Te nonbonding, while 1SA and AA crystal orbitals are Te p antibonding in a σ fashion to Cu d, but are π bonding. On the other hand 2SA, 2SS, and AS are Te p–Cu d antibonding in both a σ and π manner. Consequently, these bands lie at higher energy at the Γ point. Returning to Figure 2, 3SA is the lowest unoccupied crystal orbital at Γ, whereas AS is the highest filled one. Thus, NaCuTe is predicted to be a direct band gap semiconductor. The reason that 3SA lies so low in energy is a consequence of its nodal structure. As shown on the left side of Figure 3, it is comprised solely of Cu s atomic orbitals. Upon going from Γ to X, the *xy* glide plane is lost, whereas on going from Γ to M, the *xz* mirror plane is removed. Therefore, considerable Te s and p character mixes into this band away from the Γ point, destabilizing it. The slope in both directions of the Brillouin zone is quite steep, and this is the reason for the long tail in the DOS curve in Figure 1. Exactly the same situation applies to 3SS, which is comprised solely of Cu p_z at the Γ point.

CuTe

The structure of CuTe[6] can be rather simply derived from that of NaCuTe by a uniform contraction along the *a* axis. In CuTe $a = 3.149$ Å, $b = 4.086$ Å, and $c = 6.946$ Å, whereas in NaCuTe[13] $a = b = 4.384$ Å and $c = 7.112$ Å. A view of two layers is presented in Chart 3. Notice that there is little change in the *c* parameter. The shortest Te—Te distance between the layers is 4.39 Å, which is clearly in the van der Waals region. Using the coordinate system shown in Chart 3, the Te—Te distances within the layer and along the *x* direction are 3.15 Å. Normal covalent Te—Te bond lengths fall in the range 2.69–2.80 Å.[21] Thus, while these are rather long bonds, none the less, they lie well below the van der Waals region of 4.0–4.2 Å.[22] The Te—Te distance in the *y* direction is 4.09 Å, similar to that in NaCuTe. There are now two distinct Cu—Te bond lengths of 2.72 and 2.64 Å,

(21) (a) Pauling, L. *The Nature of The Chemical Bond*, 3rd ed.; Cornell University Press: Ithaca, NY, 1967; p 246. (b) Burns, R. C.; Gillespie, W. C.; Slim, D. R. *Inorg. Chem.* **1979**, *18*, 3086.
(22) Chauvin, R. *J. Phys. Chem.* **1992**, *96*, 9194.

Chart 3

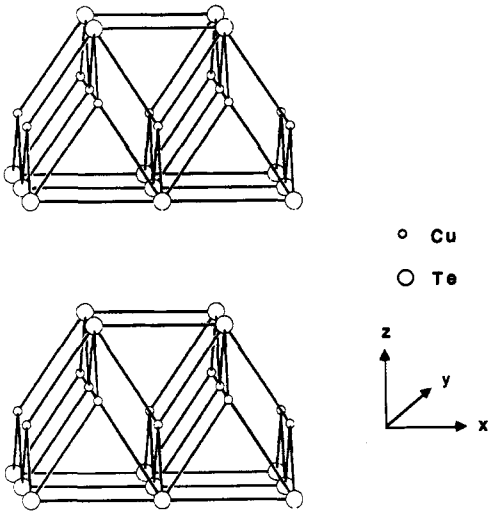

Chart 4

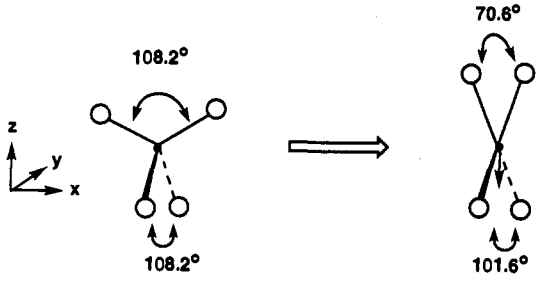

corresponding to those bonds lying along the x and y directions, respectively. The compression along the x axis causes a dramatic change in the coordination geometry around copper. As shown in Chart 4, going from NaCuTe to CuTe causes the Te—Cu—Te angle to contract by 37.6°. The copper atoms in Cu—Te no longer lie in a common plane; see Chart 3. The copper atoms are translated (Chart 4) in the z direction away from the Te—Te bonds that form along the x direction.

Figure 3 shows the orbital correlation diagram at Γ upon going from the NaCuTe to the CuTe structure for the eight bands of interest. The 1SA and 2SS crystal orbitals are pushed up to very high energies because Te—Te antibonding is increased greatly at Γ. Of course, maximal bonding occurs for these two orbitals at the X and M points, and therefore, both bands are greatly dispersed. Figure 4 compares the band dispersions from Γ to X for these orbitals in the NaCuTe and CuTe geometries. Actually, 2SS and 1SA undergo avoided crossings with the 1SS and 2SA bands, respectively, which causes both to turn upward in energy as the X point is approached. None the less, the dispersion is considerable. The 3SS and 3SA bands, derived from Cu s and p_z, are also destabilized. In the reduced symmetry Te s and p_z can now interact with both in a σ antibonding fashion, as shown on the right side of Figure 3. This intermixing also serves to stabilize 1SS and 2SA. What is not quite so apparent is that AA and AS are both slightly stabilized at Γ because of the increased π bonding between the Te p_y orbitals. At X (or M) this interaction becomes antibonding, and consequently both bands are destabilized relative to what they were for the NaCuTe geometry (see Figure 4).

We are now in a position to understand the ultimate pattern which unfolds for the DOS around the Fermi region in CuTe. Since the slope associated with AS and AA is small whereas that associated with 2SS and 1SA is large on going from Γ to X (and Γ to M), the states around the Fermi level will be comprised mostly of crystal orbitals derived from AS and AA, or as shown in Chart 5, primarily of p_y orbitals which overlap in an antibonding fashion. Figure 5 shows the DOS plot along with the projection

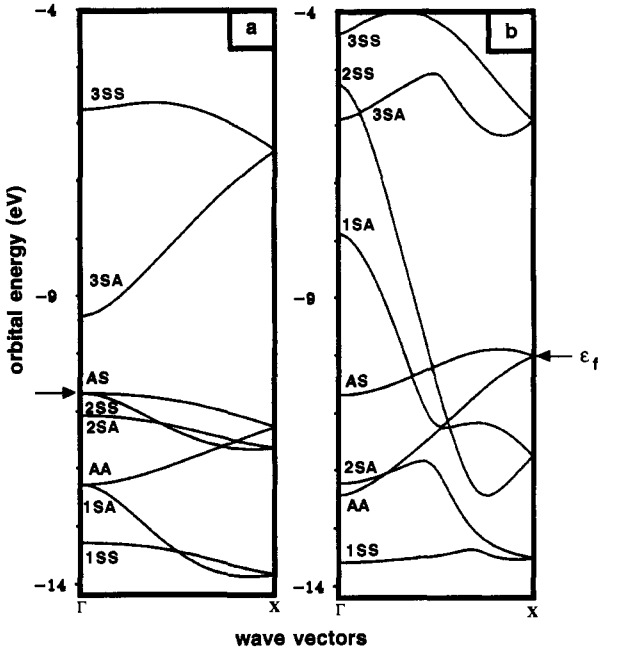

Figure 4. Comparison of the important band dispersions along Γ to X for (a) NaCuTe and (b) CuTe. The position of the Fermi level is marked by ϵ_f.

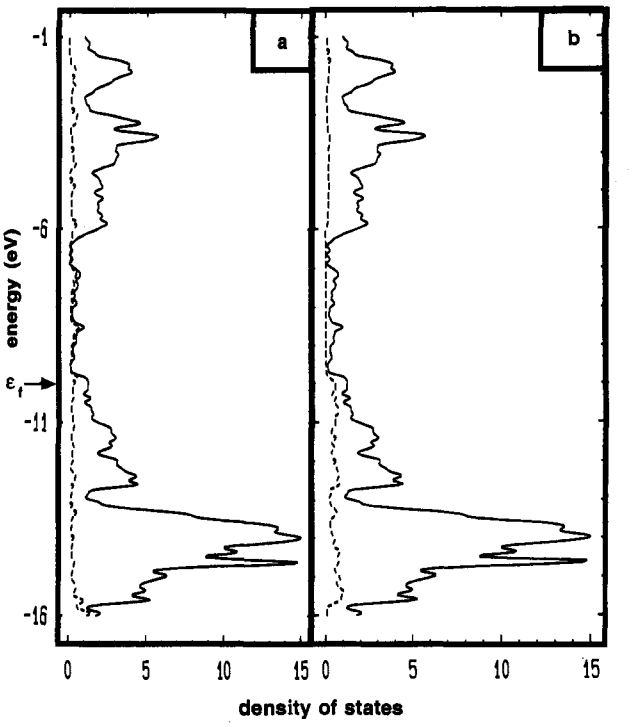

Figure 5. DOS for CuTe, where the Fermi level is indicated by ϵ_f. The projection of Te p_x is indicated by the dashed line in part a, and part b indicates the projection of Te p_y.

Chart 5

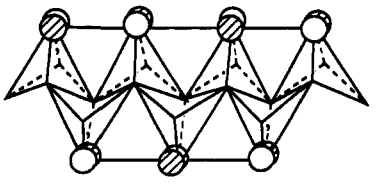

of Te p_x and p_y orbitals. The projection of Te p_x in Figure 5a shows clearly the large dispersion associated with the 1SA and 2SS bands. The Te p_y projection in Figure 5b supports the contention that the majority of states at the Fermi level (the

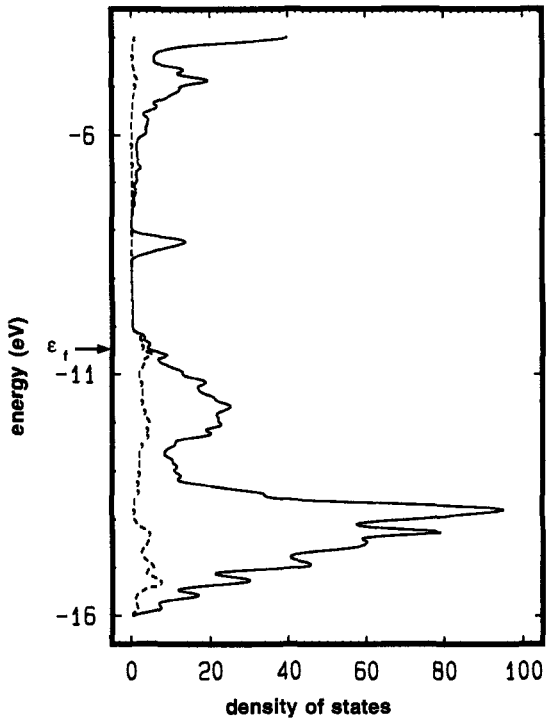

Figure 6. DOS for a single layer in $K_2Cu_5Te_5$. The Fermi level is indicated by ϵ_f, and the dashed curve is the projection of the Te p_y orbitals.

Chart 6

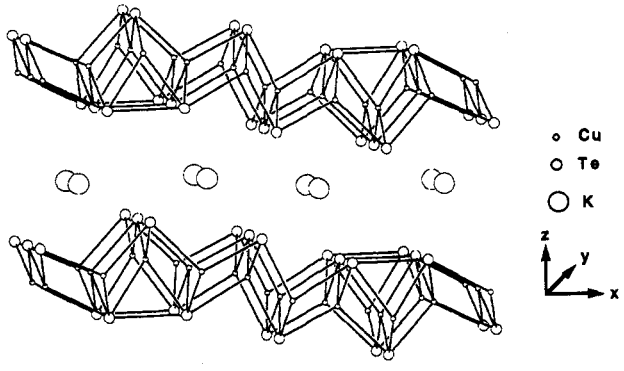

arrow at -10.0 eV) are of this type. A projection of Te p_z yields two peaks, centered at -11.4 and -12.2 eV, which lie well below the Fermi level.

It is important to realize that the compression along the *x* axis and concomitant formation of a Te—Te bonding network have not opened a band gap. CuTe is predicted to be metallic as long as the compound retains this structure. We shall examine an alternative structure for CuTe and the energetic consequences of distortion in a subsequent section.

$K_2Cu_5Te_5$

The structure of $K_2Cu_5Te_5$[14] has features that are intermediate between that of NaCuTe and CuTe. As shown in Chart 6, discrete Te—Te pairs are formed with a bond length of 2.96 Å. In contrast to NaCuTe, there now is a single layer of potassium cations; also note that a row of potassium cations (along the *y* direction; the coordinate system used is shown in Chart 6) is missing above the Te—Te bond that forms. The position of the copper atoms in the *z* direction is modulated. In common with NaCuTe and CuTe, the other Te—Te contacts both within and between Cu—Te planes are at the van der Waals limit. The total DOS is displayed in Figure 6 for $K_2Cu_5Te_5$. The region from -10.1 to -12.6 eV is primarily associated with Te p and that from -12.6 to -16.0 eV with Cu d. There is a singular peak at -8.3 eV. This corresponds to the Te—Te σ^* orbitals. There is not much dispersion since

Chart 7

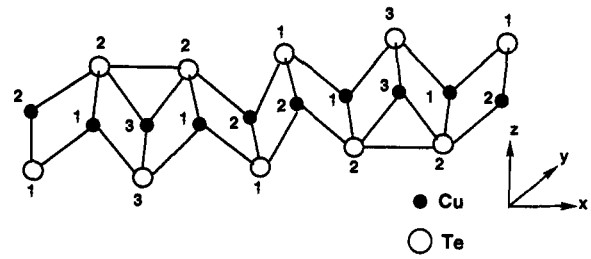

the Te—Te bonds are isolated from each other. The σ-bonding counterparts do have more dispersion as a consequence of mixing with Cu d orbitals; however, they lie in a region around -12.1 eV. With the exception of the peak at -8.3 eV, there is a large gap from -10.1 to -7.5 eV. Just as in CuTe, the Cu s states are destabilized considerably upon distortion from a tetrahedral environment. The dashed line in Figure 6 represents the projection for Te p_y. The majority of states at the Fermi level (-10.5 eV) consist of Te p_y character. Chart 7 shows the basic skeletal framework and atom-numbering system that we have employed for $K_2Cu_5Te_5$. The Te p_y occupations were Te(1) = 1.43, Te(2) = 1.45, and T(3) = 1.49 electrons. In other words, according to our calculations, the one hole per formula unit is rather uniformly delocalized over all tellurium atoms. One might have thought, by analogy to the situation in CuTe, that the Te(2)—Te(2) pairing would cause those π^* states at Te(2) to be located at a higher average energy than the p_y combinations at Te(1) and Te(3). Consequently, the holes would tend to localize on Te(2). The rationale why this does not occur in our calculations stems from the fact[14] that the Cu(2)—Te(1) and Cu(3)—Te(3) distances of 2.56 and 2.54 Å, respectively, are significantly shorter than the Cu(1)—Te(2) distances of 2.63 Å. Recall from Figure 3 that the AS orbital is Te p_y antibonding to Cu d_{yz} in a σ sense. Therefore, as the Cu(2)—Te(1) and Cu(3)—Te(3) distances become shorter, those states with Te p_y character become destabilized to an extent which is comparable to π^* in the Te(2)—Te(2) region. Thus, our calculation supports the contention that $K_2Cu_5Te_5$ is metallic. Furthermore, conductivity in the *xy* (*ac*) plane should be much greater than along the *z* (*b*) direction. Unfortuantely, crystals of $K_2Cu_5Te_5$ are thin parallelepipeds and the latter prediction cannot be checked. However, conductivity measurements parallel to the *ac* plane do reveal that $K_2Cu_5Te_5$ is a good metal (from 1.5×10^4 S cm^{-1} at room temperature to 3.2×10^5 S cm^{-1} at 5 K).[14]

The addition of one electron to $K_2Cu_5Te_5$ will just fill the DOS of the tellurium p region (to -10.1 eV in Figure 6). One might then think that $K_3Cu_5Te_5$ will be a semiconductor where potassium (or other suitable) ions have simply been inserted between the copper telluride layers. However, we feel that a structural instability may occur instead. As indicated earlier, the row of potassium ions above the Te(2)—Te(2) bond is vacant in $K_2Cu_5Te_5$. It is reasonable to suppose that this row would be filled upon going to $K_3Cu_5Te_5$. The electrostatic attraction between potassium and tellurium will be increased if the Te(2)—Te(2) bond is elongated, i.e. broken. A further energy gain will be accomplished primarily in the Cu d manifold with this distortion. The geometry around Cu(3) in $K_2Cu_5Te_5$[14] is greatly distorted from tetrahedral. The Te(2)—Cu(3)—Te(2) bond angle is only 68.6°, whereas, the bond angles around Cu(1) and Cu(2) are close to being tetrahedral. Maximal Cu—Te bonding will result from a tetrahedral geometry. Breaking the Te(2)—Te(2) bond will cause the σ^* orbitals corresponding to the peak at -8.3 eV in the DOS diagram presented in Figure 6 to fall into the tellurium p region. Therefore, $K_3Cu_5Te_5$ would remain metallic with two holes per formula unit (there are two hole states per σ^* orbital) and have a structure resembling NaCuTe.

The possibility of removing one electron from $K_2Cu_5Te_5$ to yield KCu_5Te_5 is interesting. Hypothetically, Te(1) and Te(3) could pair (to create a Te_2^{2-} unit) with the removal of the potassium

Chart 8

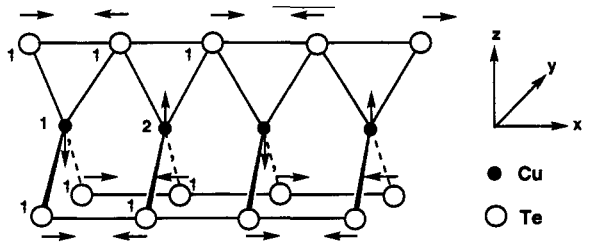

row above these atoms. This would again open a band gap. However, based on the results from the next section, the angular strain imposed on adjacent copper atoms, i.e. Cu(3) and Cu(1), may well be prohibitive. An alternative can be constructed as follows: referring to the structure in Chart 7 and starting from the left side, pair Te(1)—Te(3), remove the Te(2)—Te(2) pair, and pair Te(2)—Te(1). This will then form three Te—Te pairs per $K_2Cu_{10}Te_{10}$ unit, but two holes remain. A $K_3Cu_{10}Te_{10}$ structure akin to this is more probable since this will allow one row of potassium ions to bridge each position where Te—Te bonding is absent. Notice though that $K_3Cu_{10}Te_{10}$ will still have one hole per formula unit. The problem of potassium ion placement is apparently critical. Consider again $K_2Cu_5Te_5$ = $K_4Cu_{10}Te_{10}$, where in the absence of Te—Te bonds there are six holes. Three Te—Te bonds could be formed, in principle, with the pairing scheme described above. There are, however, only three open channels to place the potassium ions so that addition of the fourth potassium ion ruptures one Te—Te bond, which creates two holes.

The discussion above tacitly assumes that no major structural reorganization will occur, that the insertion of potassium ions will be a simple intercalation event. This may not necessarily be the case. Likewise, the use of other cations may well tolerate bridging over Te—Te bonds, and a semiconductor state may be achieved. We are left with the notion that an intermediate stoichiometry up to KCuTe will be metallic, provided that Te—Te pairing on adjacent positions is prohibitively costly in terms of angular strain. To examine this more closely, we return to CuTe itself and examine a structural variant.

CuTe Revisited

Consider CuTe to possess the NaCuTe type of structure. There is one hole (on tellurium) per formula unit. Contraction along the *a* direction does not open up a band gap; stabilization of the structure occurs certainly as a consequence of the formation of Te—Te bonding. Our hypothesis was that a further pairing distortion, shown in Chart 8 might occur. This structural distortion will pair each tellurium atom, and consequently CuTe should become a semiconductor. When we attempted to optimize a structure for CuTe akin to this, a solution was found wherein the Te—Te distances alternate along the *x* direction by 2.60 and 3.60 Å. The four Cu—Te distances vary from 2.53 to 2.87 Å, which are reasonable in comparison to those in $K_2Cu_5Te_5$.[14] Along the *x* direction in Chart 8 the Te(1)—Cu(1)—Te(1) and Te(1)—Cu(2)—Te(1) angles were 53.6° and 95.5°, respectively. The Te—Cu—Te angles in the *y* direction were 120.3°. It is clear that the geometry around copper here is even more distorted than that in the experimental geometry for CuTe.[6] The computed DOS for the paired structure is given in Figure 7. The arrow indicates the position of the highest filled orbitals. A band gap of 1.2 eV has been created. The dashed line indicates the projection of the Te p_x orbitals. Notice that the Te—Te σ orbitals are considerably dispersed in the region from −12.0 to −13.5 eV. The majority of the corresponding σ^* orbitals lie above −1.0 eV and are not shown in this figure. We calculate that the paired structure is 7.4 kcal/mol per formula unit more stable than the structure given by experiment (the experimental structure was calculated to be 0.6 kcal/mol per formula unit lower than one

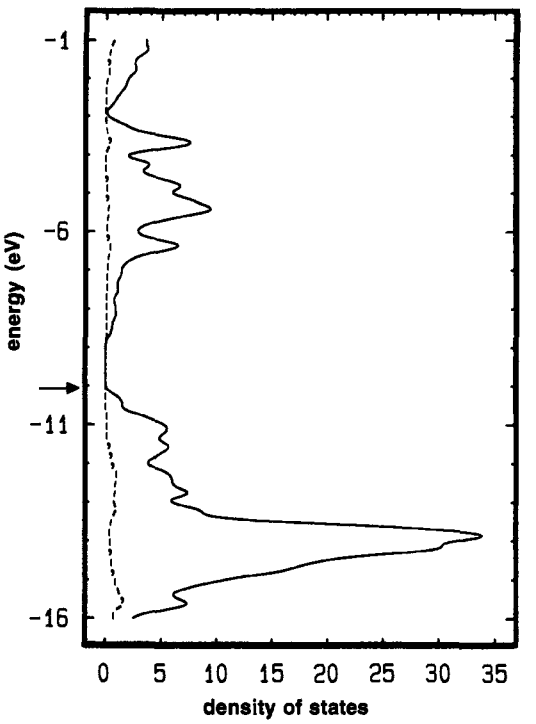

Figure 7. DOS for the paired geometry of CuTe. The arrow indicates the position of the highest filled orbitals. The dashed line indicates the projection of the Te p_x orbitals.

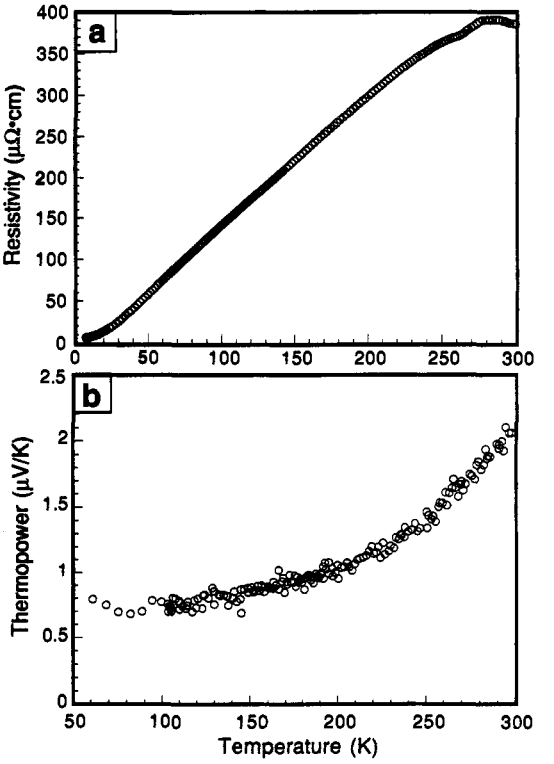

Figure 8. Single-crystal electrical resistivity (a) and thermoelectric power (b) for CuTe as a function of temperature.

with the NaCuTe structural type). This, however, is in contrast to the experimental results. Single-crystal electrical resistivity data for CuTe over a wide temperature range are shown in Figure 8a. Upon cooling to 8 K, CuTe remains metallic with no evidence for a metal–insulator transition.[23] Furthermore, the metallic character of CuTe is confirmed by the thermoelectric power measurements in Figure 8b. These data also show the absence of a phase transition and also indicate that CuTe is a p-type

(23) Zhang, X.; Kannewurf, C. R.; Kanatzidis, M. G. Unpublished results.

Chart 9

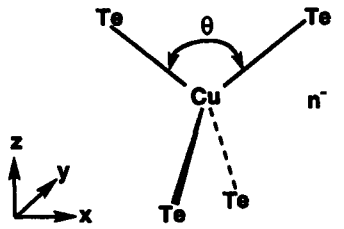

Chart 10

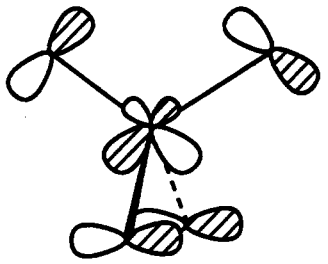

conductor. Therefore, the paired structure is not a viable option, and our extended Hückel method has proven itself to be unreliable in terms of computing relative energies for this system.

We have tried to trace the origin of this failure by carrying out several model calculations. The most simple model is a single $CuTe_4$ unit, Chart 9. For the electron-saturated $CuTe_4^{7-}$ monomer an optimal Cu—Te distance of 2.67 Å was obtained, and this is in good agreement with that in the experimental structure of NaCuTe (2.70 Å). The optimized distance in a two-dimensional $CuTe^-$ layer of NaCuTe was 2.60 Å. Thus, there is no tendency to produce abnormally short or long Cu—Te bonds using our parameter set within the extended Hückel framework. Next, angular variations from a tetrahedral to C_{2v} geometry was probed by varying θ in Chart 9.[24] For $n = 7^-$ a tetrahedral structure was produced. For the electron deficient $n = 5^-$ case (where in a formal sense, one hole exists on the two tellerium atoms) the optimal value of θ was 61.5°. This corresponds to a Te—Te bond distance of 2.86 Å. This is certainly reasonable compared to the 2.96-Å distance for the isolated Te—Te pairs in $K_2Cu_5Te_5$.[14] We parenthetically note that deformations from a tetrahedral geometry for transition metal complexes have been studied elsewhere,[25] where the driving force for distortion originates from the metal d block. Here, one member of the t_2 Te lone pair set, Chart 10, is empty for $CuTe_4^{5-}$. It evolves into a Te—Te σ^* orbital when θ is small, whereas a bonding Te—Te σ counterpart is filled and greatly stabilized. However, there is also an important restoring force. The Cu d-based e and t_2 sets in Chart 2 favor a tetrahedral geometry. It is the balance between these two forces that primarily sets the magnitude of θ and the amount of energy gain upon distortion from an electron deficient species. We submit that it is this balance which is incorrectly set in our extended Hückel calculations. By deleting the Te—Te overlap in Chart 9, the destabilization of the Cu d block was computed to be 30 kcal/mol when θ is varied from 109.47° to 61.5°. There is also actually 6 kcal/mol of stabilization due to diminishing Cu—Te π^* interaction. What is critical is that the Te—Te σ bond formation amounts to 66 kcal/mol. Therefore, the net energy gain is 42 kcal/mol. The magnitude of stabilization for the Te—Te σ bond formation appears to be suspiciously high. If this is indeed the case, then the paired structure of CuTe will be inordinately stabilized relative to the experimental one. Within the extended Hückel framework there are in fact several ways to lessen the amount of Te—Te interaction. One way is to make the Te p orbitals more diffuse. By reducing the orbital exponent by only 5%, the paired structure in CuTe becomes 5.1 kcal/mol more stable, whereas by increasing the Te p exponent by 5%, the energy difference is raised to 9.1 kcal/mol. Also the amount of intermixing between the Te and Cu d orbitals will affect this balance (greater intermixing by changing the valence-state ionization potentials can diminish Te—Te interaction). Clearly different atomic parameter sets for Cu and Te can be constructed which produce the desired energy ordering. We have chosen not to pursue this; however, we await the results of computations at a more sophisicated level than extended Hückel theory.

(24) Analogous computations were performed on a linear chain trimer, $Cu_3Te_{10}^{17-}$ and $Cu_3Te_{10}^{15-}$, which produce very similar results and are not reported here.

(25) (a) Summerville, R. H.; Hoffmann, R. *J. Am. Chem. Soc.* **1976**, *98*, 7240. (b) Sherwood, P.; Hoffmann, R. *Inorg. Chem.* **1989**, *28*, 509.

Table 1. Atomic Parameters Used for the Calculations

	orbital	H_{ii}(eV)	ζ_1	ζ_2	C_1[a]	C_2[a]
Cu	4s	−11.40	2.20			
	4p	−6.60	2.20			
	4d	−14.00	5.95	2.10	0.6096	0.5843
Te	5s	−21.20	2.51			
	5p	−12.50	2.16			

[a] Contraction coefficients used in the double-ζ expansion.

Acknowledgment. We thank the Robert A. Welch Foundation, the Petroleum Research Fund as administered by the American Chemical Society, the Texas Center for Superconductivity at the University of Houston (Prime Grant MDA 972-88-G-002 from the Defense Advanced Research Projects Agency and the State of Texas), and the University of Houston President's Research Enhancement Fund for support of this work. Financial support from the National Science Foundation, DMR-9202428, is gratefully acknowledged. We thank Professor C. R. Kannewurf for electrical measurements. We also thank the NSF for a generous allocation of computer time at the Pittsburgh Superconducting Center.

Appendix

Extended Hückel calculations[21] with a modified Wolfsberg–Helmholz formula[26] have been used. The atomic parameters[27] are listed in Table 1. The geometrical details of the calculations were taken from the experimental structures. For the two-dimensional property calculations a 120K point set was used for CuTe and NaCuTe, whereas a 96K point set was used for $K_2Cu_5Te_5$. A 350K point set was used for the band structure calculations on CuTe and NaCuTe.

(26) Ammeter, J. H.; Burgi, H.-B.; Thiebeault, J. C.; Hoffmann, R. *J. Am. Chem. Soc.* **1978**, *100*, 3686.

(27) Hay, P. J.; Thibeault, J. C.; Hoffmann, R. *J. Am. Chem. Soc.* **1975**, *97*, 4884. Hughbanks, T. Private communication.